

Electronic Supplementary Information for

Defect Healing in Two-Step Deposited Perovskite Solar Cells via Formamidinium Iodide Compensation

Chenguang Xin^{a,b#}, Jiangbin Zhang^{c,d,e#}, Xin Zhou^{a,b#}, Linchuan Ma^f, Fuhua Hou^{a,b}, Biao Shi^{a,b}, Sanjiang Pan^{a,b}, Bingbing Chen^{a,b}, Pengyang Wang^{a,b}, Dekun Zhang^{a,b}, Xinliang Chen^{a,b}, Ying Zhao^{a,b}, Artem A. Bakulin^d, Yuelong Li^{*a,b}, Xiaodan Zhang^{*a,b}

^aInstitute of Photoelectronic Thin Film Devices and Technology of Nankai University, Key Laboratory of Photoelectronic Thin Film Devices and Technology of Tianjin, Solar Energy Research Center of Nankai University, #38 Tongyan Road, Jinnan District, Tianjin 300350, P. R. China.

^b Collaborative Innovation Center of Chemical Science and Engineering, Renewable Energy Conversion and Storage Center of Nankai University, #94 Weijin Road, Nankai District, Tianjin 300072, P. R. China.

^c Cavendish Laboratory, University of Cambridge, J J Thomson Avenue, Cambridge, CB3 0HE, United Kingdom.

^d Department of Chemistry, Imperial College London, South Kensington Campus, London SW7 2AZ, United Kingdom.

^e College of Advanced Interdisciplinary Studies, National University of Defense Technology, Changsha 410073, P. R. China.

^f Electronic Information Laboratorial Teaching Center, Nankai University, #38 Tongyan Road, Jinnan

District, Tianjin 300350, P. R. China.

*Corresponding author:

Prof. Yuelong Li, lyl@nankai.edu.cn, Tel.: +86-22-85358845; Fax: +86-22-23499304

Prof. Xiaodan Zhang, xdzhang@nankai.edu.cn, Tel.: +86-22-85358082; Fax: +86-22-23499304

These authors contribute equally to this work

Experimental: in the page of S3

Figure: Fig. S1-S7 in the Page S5-S9

Table: Table S1 in the page of S10

1. Experimental Section

Materials: All the chemicals and solvents were used as received without further modifying. The SnO₂ colloid precursor was obtained from Alfa Aesar (Tin (IV) oxide). Isopropyl alcohol (IPA), N,N-dimethyl formamide (DMF), and dimethyl sulfoxide (DMSO) were purchased from Alfa Aesar. FAI, methylammonium bromide (MABr), and methylammonium chloride (MACl) were bought from Shanghai Materwin New Materials Co.,Ltd. The 1.3M PbI₂ precursor solution was dissolved in anhydrous DMF:DMSO (9:1=v/v). After PbI₂ had cooled down to room temperature, the organic salt solution of FAI:MABr:MACl (60 mg:6 mg:6 mg dissolved in 1 mL IPA). The hole transporting layer solution was prepared by dissolving Spiro-OMeTAD (80 mg), tBP (28.5 μ L) and Li-TFSI (35 μ L) solution (260 mg Li-TFSI in 1 mL acetonitrile) in 1 mL chlorobenzene.

Device fabrication: ITO glass was sequentially cleaned in detergent, acetone, isopropanol and deionized water before using, the ITO was cleaned by UVO for 20 min. Then, the SnO₂ nanoparticle film (2.5%) was spin-coated at 4000 rpm for 30 s, and annealed in ambient air at 150 °C for 30 min. After that, the 1.3M PbI₂ precursor solution was spin-coated at 1500 rpm for 30s onto SnO₂ surface, followed by annealing at 70 °C for 1 min. Then, the organic salt solution was deposited onto the PbI₂ film at 1500 rpm for 30 s, and annealed at 150 °C for 15 min in ambient air (50% humidity). For the FAI healing treatment, different concentration of FAI solution in IPA (from 0 to 5 mg/mL) was added on the perovskite film, and instantly spin coated at 1500 rpm for 30 s, and annealed at 150 °C for 3 min in N₂ filled glove box. The Spiro-OMeTAD solution was spin-casted on the perovskite film at 4000 rpm for 30 s. Finally, 80 nm Au counter electrode was deposited by thermal evaporation using a shadow mask.

Characterizations: The morphology of the perovskite films were characterized by field-emission SEM

(JEOL JSM-7800F) and AFM (SPA-400). XRD patterns were measured by X-ray diffraction (Rigaku ATX-XRD) with Cu K α radiation ($k = 1.5405 \text{ \AA}$) at $10^\circ \text{ min}^{-1}$. The optical characteristics spectra were measured with UV–Vis–NIR spectrophotometer (Cary 5000) in the wavelength from 300 nm to 900 nm at room temperature.

Photocurrent density-voltage (J-V) curves were measured under AM 1.5G 1 sun (100 mW/cm^2) illumination by a solar simulator (HAL-320, ASAHI SPECTRA Co. Ltd., Japan) equipped with a Xenon light. The calibrated light was carried out by a detector (CS-20, ASAHI SPECTRA Co. Ltd., Japan) with silicon reference cell. Photocurrent density-voltage (J-V) curves of solar cells were measured at 25°C . The scanning step was 40 mV for the J–V curve measurement. Unless specified, bias scan from 1.2 V to -0.2 V firstly (reverse scan) and return back (forward scan) with a delay time of 50 ms. The trap density was calculated according to the space-charge limited current (SCLC) method. All devices were measured in the dark from 0 to 5.0 V with a scanning step of 20 mV. The observed response was analyzed according to SCLC theory. A metal mask with a window of 0.1 cm^2 was covered on the light illumination side to define the active area of the cell. The spectral response was taken by an external quantum efficiency (EQE) measurement system (QEX10, PV Measurement) with a scanning step of 10 nm. The xenon arc lamp was used as the monochromatic light excitation source and filtered by a double grating. Photoluminescence (PL) and time-resolved photoluminescence (TRPL) measurement were performed by a spectrometer (Edinburgh FS5) at room temperature with laser wavelength and lifetime of 475 nm and 1000 ns, respectively. The XPS spectra were taken on the Thermo Scientific ESCALAB 250Xi. CLSM images were visualized by using confocal laser scanning microscopy (Leica TCS SP8) with an excitation wavelength at 488 nm. All confocal images were acquired using a $63 \times 1.4 \text{ NA}$ oil-immersion objective lens.

Transient absorption. 532 nm light at 1 kHz from Nd:YVO₄ laser (AOT-YVO-25QSPX, Advanced Optical Technologies) was chopped to 500 Hz (MC2000B, Thorlabs) and acted as the pump light. The probe light initially came from a Ti:sapphire amplifier (Solstice Ace, Spectra Physics) operating at 1 kHz. Nonlinear optical parametric amplifier using a β -barium borate crystal was adopted to obtain broadband amplification of the seed light from a thin sapphire glass. Part of the probe light was monitored as a reference to account for shot-to-shot variation of laser lights. After the beams were focused into a spectrometer (Shamrock SR 303i, Andor), the signal was detected using a pair of linear image sensors (G11608, Hamamatsu) and read out with a custom-built board (Stresing Entwicklungsburo).

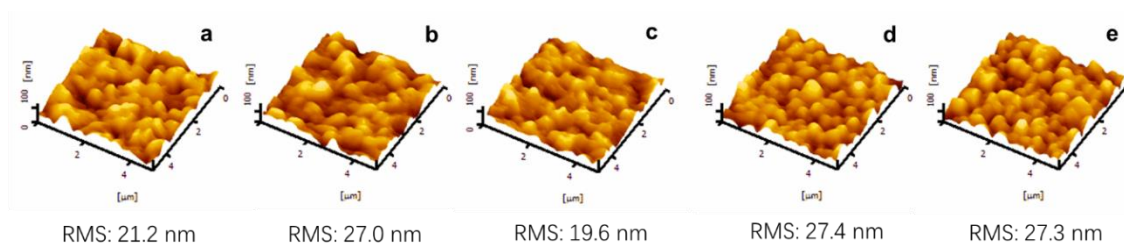


Figure S1 Atomic force microscopy images of perovskite films post-treated with different concentration of FAI in IPA: the control sample in (a), pure IPA or 0 mg/mL in (b), 1 mg/mL in (c), 3 mg/mL in (d) and 5 mg/mL in (e), respectively. “RMS” stands for the root mean squared roughness.

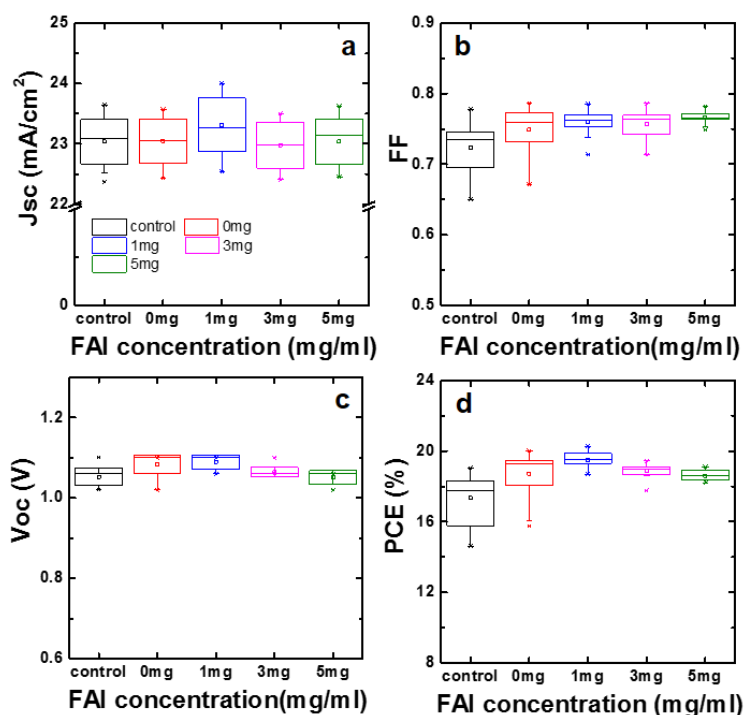


Figure S2 Graphs comparing photovoltaic properties of perovskite solar cells with varied concentration of FAI in IPA: J_{sc} in (a), FF in (b), V_{oc} in (c) and PCE in (d), respectively. The statistics is based on at least 15 cells from different batches for each conditions.

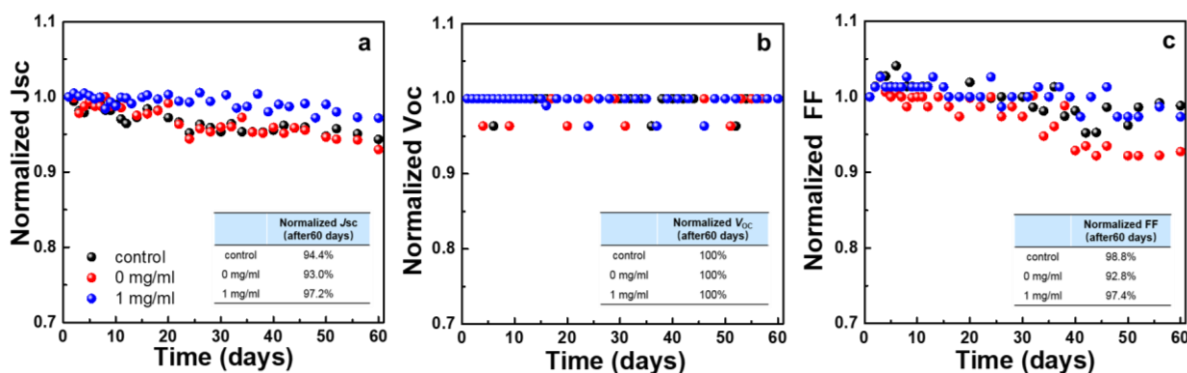


Figure S3. The long-term stability of the control, IPA and FAI healed PSCs with normalized photovoltaic parameters: J_{sc} in (a), V_{oc} in (b) and FF in (c). The device performance was continuously measured for 60 days during the storage in a N_2 environment.

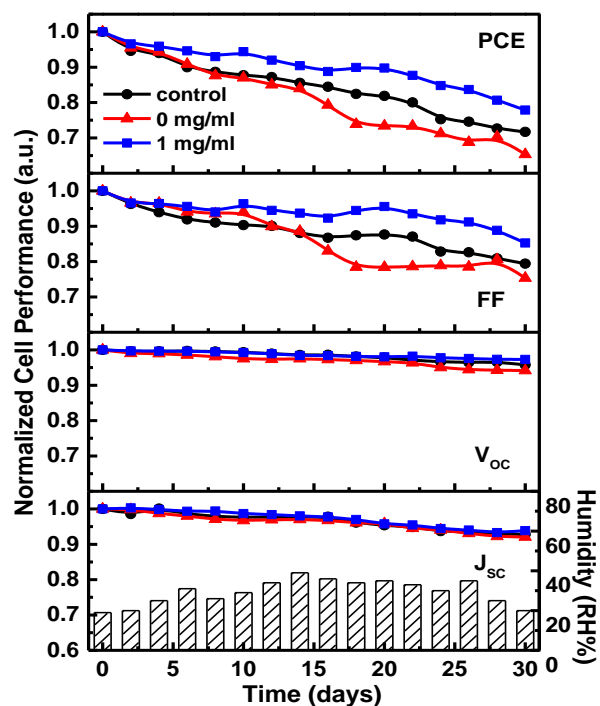


Figure S4 Long-term stability of perovskite solar cells under ambient with varied humidity. All devices are measured without encapsulation but stored in the air for 30 days at room temperature and in the dark. For each condition, at least ten devices were monitored continuously and the results were averaged.

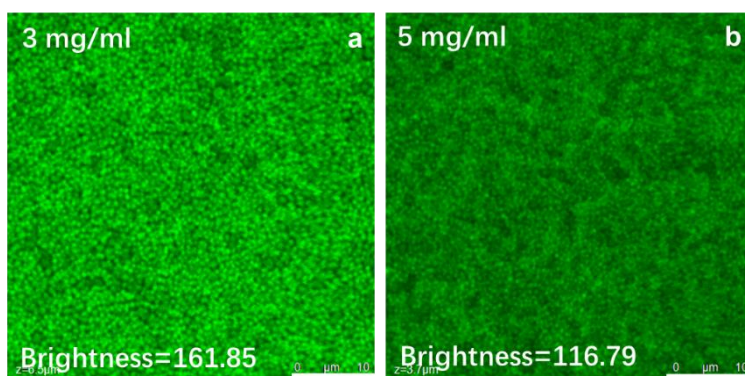


Figure S5 Confocal laser scanning microscopy (CLSM) images of perovskite films treated with 3 mg/mL and 5 mg/mL FAI in IPA.

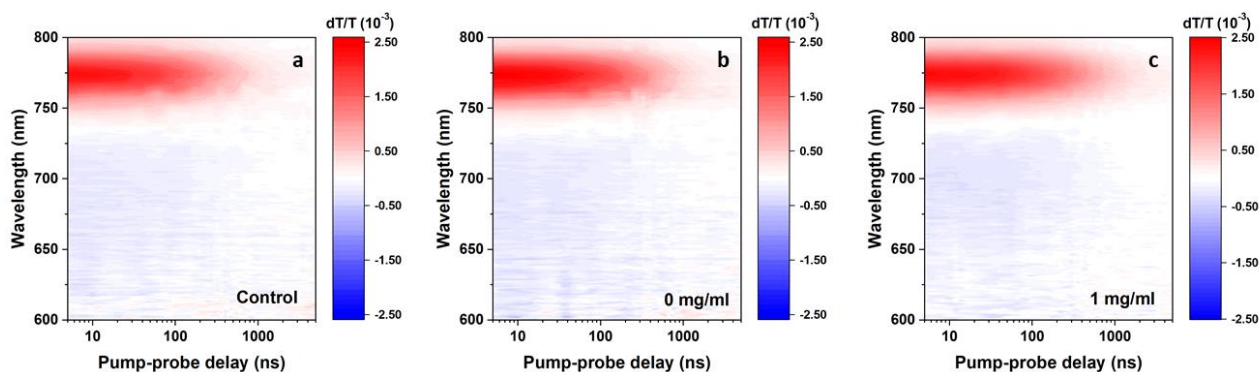


Figure S6 The transient absorption 2D map of the samples of the control, 0 mg/mL FAI and 1 mg/mL FAI.

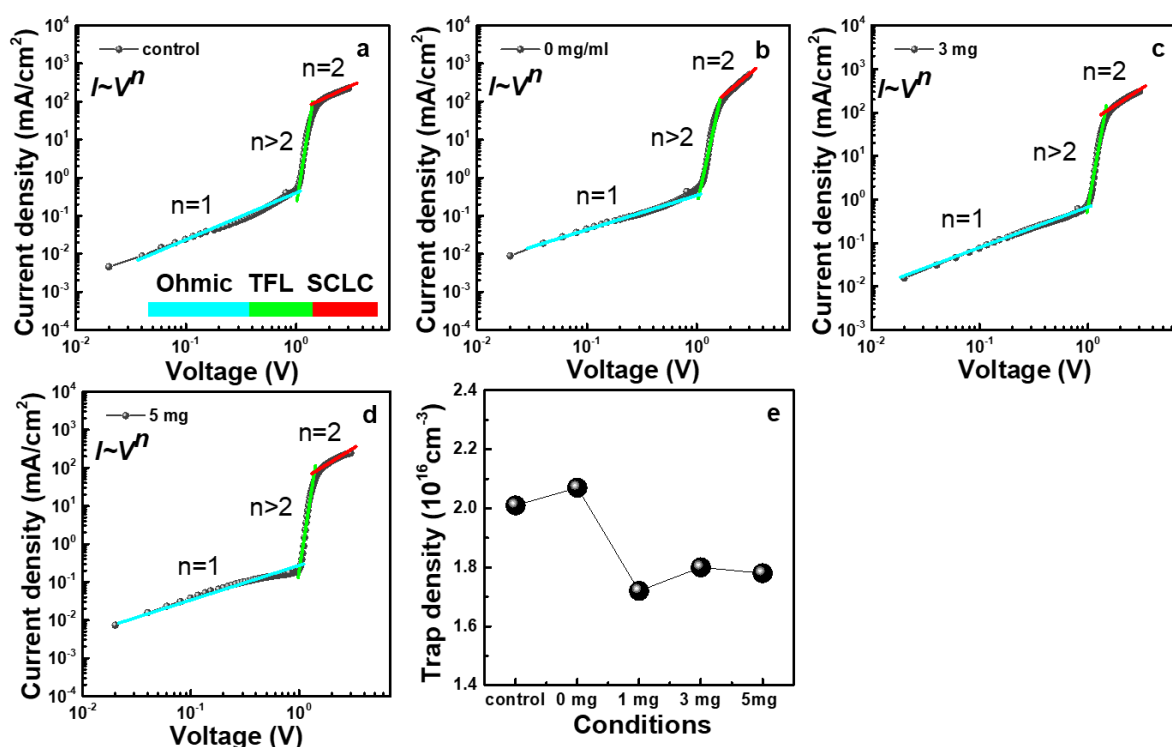


Figure S7 Space charge limited current (SCLC) measurements of perovskite films of the control in (a) or treated by 0 mg/mL FAI/IPA in (b), 3 mg/mL FAI/IPA in (c), 5 mg/mL FAI/IPA in (d) and the plot of trap density under different healing conditions in (e).

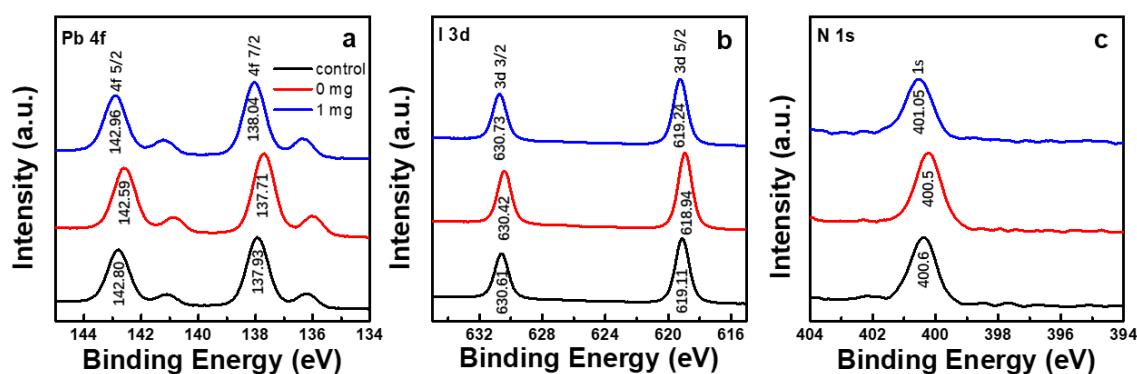


Figure S8. XPS spectra of Pb 4f in (a), I 3d in (b) and N 1s in (c).

A surface-sensitive X-Ray photoelectron spectroscopy (XPS) was used to observe the evolution of chemical states and film composition in **Figure S8**. The chemical states of Pb, I and N atoms were detected. Considering that the chemical states of Pb and I atoms in PbI_2 and perovskite are similar, it is hard to distinguish whether the Pb and I signals are from either the PbI_2 phase or the perovskite phase.

The XPS spectrum of Pb (4f) in both of the composition show a doublet due to spin–orbit splitting with the two possible states Pb (4f)_{5/2} and Pb (4f)_{7/2} having binding energies 142.80 eV and 137.93 eV, respectively for control, 142.59 eV and 137.71 eV for 0 mg, 142.96 eV and 138.04 eV for 1 mg (Figure 5a). This difference in binding energy for Pb (4f)_{5/2} and Pb (4f)_{7/2} peak may be assigned to the residual PbI_2 due to IPA treatment in agreement with previous XRD data. Likewise, XPS spectrum of I (3d) in both of the composition show spin–orbit splitting with two possible states I (3d)_{3/2} and I(3d)_{5/2} having binding energies 630.61 eV and 619.11 eV for control, 630.42 eV and 618.94 eV for 0 mg and 630.73 eV and 619.24 eV for 1 mg. Again, the difference in binding energy for I (3d)_{3/2} and I (3d)_{5/2} peak can account for the change in the chemical environment of I due to IPA treatment.

Table S1 Fitted parameters of decay curves at 780-790 nm with two exponential components and its average lifetime from transient absorption measurements.

Sample	A₁	τ_1 (ns)	A₂	τ_2 (ns)	τ_{ave} (ns)
Control	0.738	278.42	0.257	2097	1595.0
0 mg/mL	0.724	218.81	0.285	2017	1628.5
1 mg/mL	0.699	304.20	0.300	2387	1910.1